

10B.7 EVOLUTION OF MESOSCALE CONVECTIVE SYSTEMS DURING TROPICAL CYCLONE FORMATIONS IN THE WESTERN NORTH PACIFIC

Jenny S. N. Hui¹, Kevin K. W. Cheung², Cheng-Shang Lee^{1*} and Russell L. Elsberry³

¹Department of Atmospheric Sciences, National Taiwan University

²National Science and Technology Center for Disaster Reduction, Taiwan

³Department of Meteorology, Naval Postgraduate School, Monterey, California

1. Introduction

Recent modeling studies (e.g., Montgomery et al. 2006) indicate that mesoscale and even convective-scale processes are essential during tropical cyclone (TC) formations. Whereas detailed diagnosis on these mesoscale and convective-scale systems can be performed based on the model simulation results, their existence and role played during formations have to be validated by observations. One recent example is Reasor et al. (2005) that confirms the presence of lower-to-middle tropospheric mesoscale cyclonic circulations and their interaction during the formation of Atlantic Hurricane Dolly (1996). TC formations occur in data-sparse ocean regions with little traditional observations. However, with growing number of remote-sensing platforms (satellite imagery, microwave channels, GPS sounding, etc.) and derived products (e.g., cloud-drift winds and derived moisture), there are opportunities to study the detailed mesoscale processes during TC formations based on these new observations, and for guiding the directions of further numerical simulation studies.

This study is an extension of Ritchie and Holland (1999) and Cheung and Elsberry (2004) in identifying the existence (or not) of mesoscale convective systems (MCSs) and their potential contributions during TC formations in the western North Pacific (WNP). The hypothesis is that mesoscale features such as MCSs determine the position and timing of TC formations within generally favorable environmental conditions.

2. Data and Cases Classification

Infrared channel-1 (IR1) satellite imagery from GMS-5 and GOES-9 that cover the area 0-22°N, 90°-160°E (obtained from the archive of Kochi University, Japan) are used to monitor the convective activities during TC formations. For surface features, both the 25-km resolution swath data and 50-km resolution gridded data of the QuikSCAT oceanic winds are used. In addition, analyses from the European Center for Medium-range Weather Forecast (ECMWF) are utilized to extract large-scale environmental parameters during TC formations.

A total of 124 TC formations in the WNP during September 1999–December 2004 are examined. MCSs two days before the TC formation alert was issued for each case are identified by the deep-convective areas (IR1 temperature < 214 K with an

area greater than 4×10^4 km² and eccentricity > 0.5) in the GMS-5/GOES-9 satellite imagery.

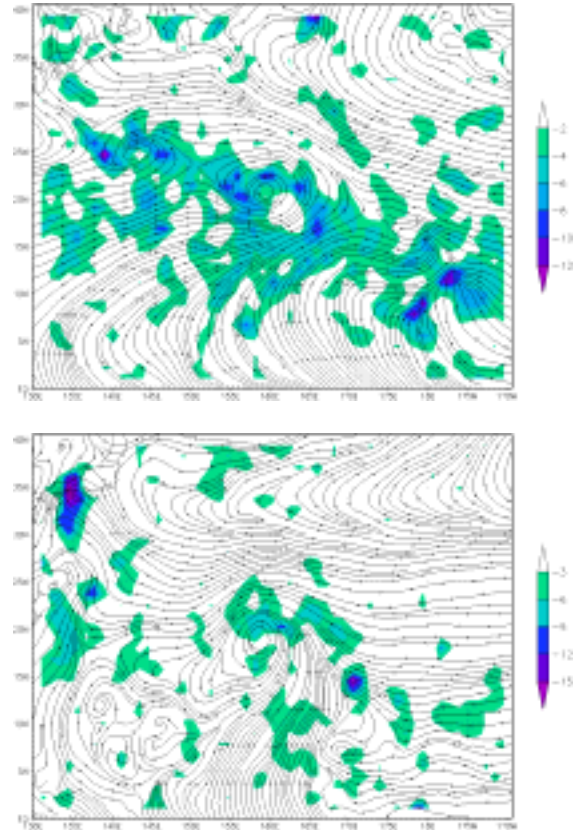


Fig. 1 Composite 850-hPa flow of the monsoon confluence (MC, upper panel) and easterly wave (EW, lower panel) formation pattern using ECMWF analyses. The shaded contours indicate divergence.

For diagnosing different mechanisms of formation, the 124 cases are classified into six categories according to their large-scale formation patterns: monsoon shear (MS, 30 cases), monsoon confluence (MC, 23 cases), southwesterly flow (SW, 23 cases), southwesterly and northeasterly flow (SW-NE, 19 cases), trade wind northeasterly flow (NE, 19 cases), and easterly wave (EW, 10 cases). These patterns are defined based on 850-hPa and 925-hPa flows because the near-surface winds are much affected by surface friction. The composite MC

* Corresponding author address: Cheng-Shang Lee, Department of Atmospheric Sciences, National Taiwan University, 1, Sec 4, Roosevelt Road, Taipei 106, Taiwan ROC; email: cslee@nat.as.ntu.edu.tw

pattern in which the southwesterlies meet the easterlies near the system center and that of the EW pattern are shown in Fig. 1. The classification here is similar to but not exactly the same as that in Ritchie and Holland (1999). In particular, the monsoon environment is further classified into categories according to specific large-scale forcing (the SW, NE and SW-NE patterns). It is found that different patterns of MCS evolution exist for these categories and therefore the fine classification may be helpful in identifying more detailed physical processes during the mesoscale interactions.

3. MCS Activities during TC Formations

The duration of development from tropical disturbances to a TC usually ranges from several hours to more than two days. It is likely the convective behavior during TC formations is altered by the diurnal cycle and it is an important factor to consider when examining the deepness of convection in MCSs. The composite (using all 124 cases) IR temperature variation according to local times during the day in the vicinity of the TC formations shows that the difference between convection maximum and minimum is about 5 °C in a diurnal cycle (Fig. 2). Accordingly, the fractional area of deep convection in a day also shows similar variation. Thus, this temperature difference has to be taken into account when examining the subsequent temperature profiles of individual TC formations.

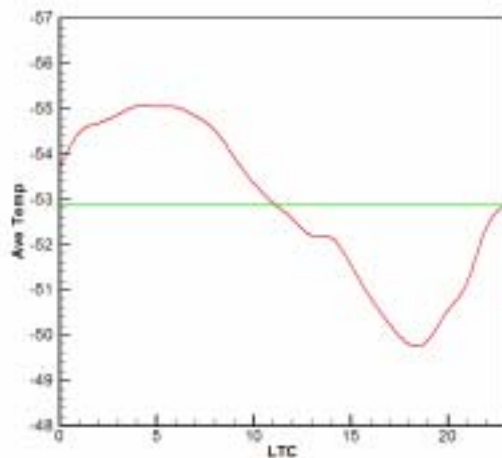


Fig. 2 Composite IR temperature (°C) for all the 124 TC formation cases showing the diurnal cycle of convection within 24 h of local time (LTC).

Whereas MCSs activities are much affected by the diurnal variation, one to several MCSs are identified in most of the 124 formations in this study. On average, more MCSs are found 48 h before formation in the monsoon-related patterns (MS, SW, SW-NE, and NE), whereas in the EW pattern only one MCS is identified in almost every formation and the MCS only appeared within 24 h prior to formation and usually developed until the formation time (Table 1). The mean lifetime of the MCS embedded in easterly

waves (5.5 h) is also much shorter than that in other formation patterns.

In some of the formation cases, successive developments of MCS occurred that may contribute to the formation process at multiple times. For the 5-year period in this study, the overall percentage of cases with MCSs at multiple times is 69% (Table 2). On the other hand, 39% of the cases have more than one MCS coexisting at a single time. Note that these two percentages are close to those in the study of Ritchie and Holland (70% and 44% respectively). The percentages for individual formation patterns indicate that the MS pattern is the most favorable for generating more than one MCS during formation. The monsoon-related patterns as well as monsoon confluence are also quite favorable for generating multiple MCSs. Comparatively, as there is only one MCS identified in almost all cases in the EW pattern, so that both percentages in this category are low.

| Large-scale flow pattern | Mean number of MCSs | Mean life time of MCSs (h) |
|--------------------------|---------------------|----------------------------|
| MS | 2.1 | 13.3 |
| MC | 1.7 | 11.8 |
| SW | 1.6 | 11.7 |
| SW-NE | 1.3 | 12.7 |
| NE | 1.6 | 14.6 |
| EW | 0.9 | 5.5 |

Table 1 Mean number and lifetime of the MCSs identified in the six formation patterns.

| Large-scale flow pattern | MCSs at multiple times | Multiple MCSs at a single time |
|--------------------------|------------------------|--------------------------------|
| MS | 88% | 44% |
| MC | 73% | 47% |
| SW | 63% | 44% |
| SW-NE | 58% | 39% |
| NE | 72% | 36% |
| EW | 40% | 10% |
| Total | 69% | 39% |

Table 2 Percentage of cases in each of the six formation patterns with MCSs at multiple times and multiple MCSs at a single time.

4. Characteristics of Convection

Besides identifying the MCSs, the general convective characteristics during formation of the 124 cases are also examined by looking at the percentage of deep convection area in the vicinity of formation and the actual IR temperature. For example, the percentages of deep convection (with IR temperature < -60°C) area one day before formation for different large-scale patterns in different domain sizes centered on the system show that in the MC pattern the deep convection is concentrated in relatively small area (Table 3). For other monsoon-related patterns, the percentage of deep convection is around 20-30% within 200 km from the center. For the EW formation pattern, the fact that percentage of deep convection area is decreasing rapidly for larger domain sizes indicates that the convection associated with the MCS in this pattern is very near to the center.

Examination of the average IR temperature one day before formation in circular domains again distinguishes the EW pattern from the others (Table 4). Whereas the average temperature in the monsoon-related patterns is usually lower than -20°C , that for the EW pattern is much higher. This indicates that the convection in the easterly waves is not as deep as in the other patterns, which may be a result of different strengths in the large-scale forcing. In general, the locations of the deep convection are found to be well correlated with the low-level forcing. More detailed analysis of the data is being carried out to investigate how the MCS development provides feedback to the large-scale forcing, and their relative importance of MCSs in the different formation patterns.

| Domain Size | EW | NE | NESW | MC | MS | SW |
|-------------|------|------|------|------|------|------|
| 200 km | 24.4 | 25.1 | 25.8 | 13.9 | 29.5 | 27.7 |
| 400 km | 16.9 | 23.4 | 23.5 | 16.1 | 24.3 | 23.1 |
| 600 km | 12.0 | 19.8 | 19.0 | 15.6 | 19.8 | 18.6 |
| 800 km | 9.3 | 16.5 | 15.8 | 13.9 | 15.9 | 15.8 |

Table 3 Percentage of deep convection (IR temperature $< -60^{\circ}\text{C}$) area in different domain sizes centered on the system for the six formation patterns.

| Radius ($^{\circ}$ lat) | EW | NE | NESW | MC | MS | SW |
|--------------------------|-------|-------|-------|-------|-------|-------|
| 1° | -15.5 | -24.7 | -29.9 | -27.5 | -26.3 | -21.0 |
| 2° | -12.3 | -23.6 | -27.0 | -26.5 | -23.5 | -19.5 |
| 3° | -8.8 | -21.9 | -23.8 | -24.4 | -20.5 | -17.8 |
| 4° | -5.6 | -20.0 | -21.0 | -22.1 | -18.0 | -15.7 |

Table 4 Average IR temperature in circular domains with different radii for the six formation patterns.

In addition, the temporal profiles of convection before formation are also examined. Preliminary results indicate that several characteristic temporal profiles exist that seem to be more complicated than the well-known two-stage process found in Zehr (1992). For example, there are cases with multiple deep convection within 48 h before formation (Fig. 3 upper panel) and in a few cases the average temperature actually increases during formation (Fig. 3 lower panel).

5. Summary

This study diagnoses the contribution of MCSs to TC formation by examining 124 cases in the WNP during 1999–2004 based on satellite data. At least one MCS is found in almost all the cases, and some large-scale synoptic patterns (e.g., the monsoon related) are more favorable for MCS development. In some others (e.g., easterly wave), deep convection may concentrate near the system center. Moreover, some characteristic profiles of convection two days before formation are identified.

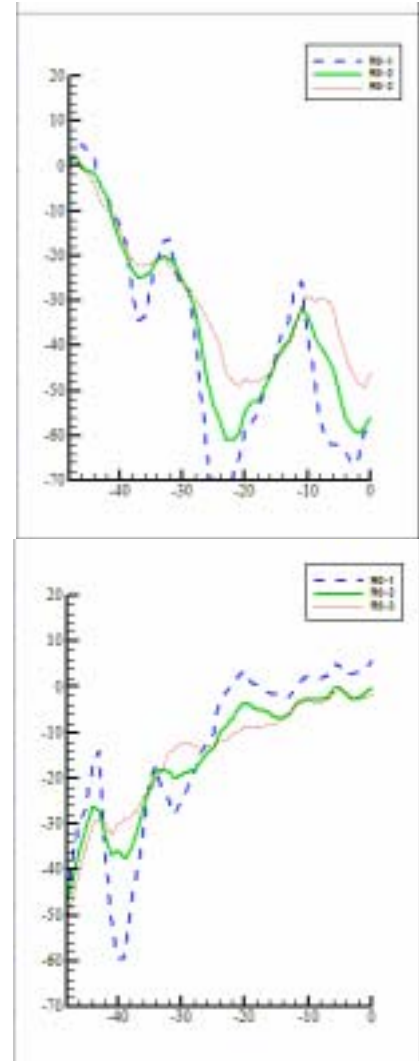


Fig. 3 Examples of IR temperature profile ($^{\circ}\text{C}$) 48 h before formation averaged within 1° (R0-1), 2° (R0-2) and 3° (R0-3) lat. from center.

Acknowledgments

This research is partially supported by the National Science Council of Taiwan, R.O.C.

References

- Cheung, K. K. W., and R. L. Elsberry, 2004: Characteristic fields associated with tropical cyclone formations. *Preprints, 26th Conf. Hurr. Trop. Meteor., Miami*, Amer. Meteor. Soc., 48–49.
- Montgomery, M. T., M. E. Nicholls, T. A. Cram, and A. B. Saunders, 2006: A vortical hot tower route to tropical cyclogenesis. *J. Atmos. Sci.*, **63**, 355–386.
- Reasor, P. D., M. T. Montgomery, and L. F. Bosart, 2005: Mesoscale observations of the genesis of Hurricane Dolly (1996). *J. Atmos. Sci.*, **62**, 3151–3171.
- Ritchie, E. A., and G. J. Holland, 1999: Large-scale patterns associated with tropical cyclogenesis in the western Pacific. *Mon. Wea. Rev.*, **127**, 2027–2043.
- Zehr, R. M., 1992: Tropical cyclogenesis in the western North Pacific. NOAA Tech. Rep. NESDIS 61, 181 pp.